COBEM 2021 26th International Congress of Mechanical Engineering
November 22-26, 2021, Virtual Congress, Brazil
ABCM Associação Brasileira de Engenharia e Ciências Mecânicas

COBEM2021-1632
DESIGN OPTIMIZATION FOR BASE EXCITATION PROBLEM OF A CANTILEVERED BEAM COUPLED WITH SHUNT CIRCUIT ON FATIGUE ANALYSIS

João Pedro Sena
Gutembergy Ferreira Diniz
Antônio Marcos Gonçalves de Lima
Erivaldo Pereira Nunes
Marcelo Araújo Delgado Filho
Unversidade Federal de Uberlândia, Av. João Naves de Ávila, 2121 - Santa Mônica, Uberlândia - MG, 38408-100
sena.joaopedro42@gmail.com
gutembergy_ferreira@hotmail.com
amglima@ufu.br
erivaldo_pn@yahoo.com.br
marcelo.delgado@ufu.br

Abstract. *Mechanical structures, in various applications, may be subjected to operational or ambient vibration. The vibration generates stresses in the structure, accumulating through time and resulting in cracks or even structural failures. Vibration control studies date back to the last century and present a variety of alternatives in order to attenuate the vibration and therefore the accumulating stresses. A simple Euler-Bernoulli formulation was used to calculate the stress history and the Frequency Response Function of the tip displacement in a cantilever beam. Parameterization of the formulation to a single function was performed to enable the use of a Genetic Algorithm and the minimize the peak value, obtaining then the optimal resistance. This resistance was then used to obtain the stress history of the beam, to calculate the accumulated damage and to define the fatigue life in the given conditions. The results show the optimal resistance value as the configuration with the highest fatigue life.*

Keywords: *Shunt Circuits, Optimization, Fatigue, Dynamic Systems, Cantilever-beam*

1. INTRODUCTION

It is widely known that mechanical structures, in the most varied engineering applications, can be subject to vibrations induced by operational or environmental effects. Unwanted vibrations are harmful to the structures since they cause fatigue and, consequently, the premature wear of mechanical components, which can cause catastrophic losses. In this way, different concepts of vibration control systems have been studied and proposed over the years (Wright and Kidner, 2004; Gripp and Rade, 2018)

A variety of active, passive and hybrid vibration and noise control techniques have been developed and consolidated (Vér and Beranek, 2005). However, the demand for increasingly lightweight structures requires new vibration control technologies and, therefore, new solutions are constantly have been sought. In this context, intelligent materials have emerged as innovative solutions.Those materials are known for the ability to couple between differents physical domains (thermal, electrical, mechanical, chemical), where the response of variables to a given physical domain can be modified to changes the variables of another domain (Leo, 2007).

Among the smart materials with practical interest, the piezoeletric materials are those with the most widespread applications. In fact, these materials can be used as sensors and actuators coupling the mechanical and electrical domains, can be found with a broad range of mechanical characteristics, ranging from very stiff ceramics to flexible and light polymers, and can operate in a wide frequency range (Gripp and Rade, 2018).

Several works describe the use of piezoeletric material coupled with a shunt circuit to achieve vibration control. Gotz *et al.* (2017) studied the effects on the attenuation of a beam's lateral vibrations, in which depends on the adequate tuning of the shunt circuit. In other study, Hansson *et al.* (2004) developed a new method to reduce vertical flexural vibrations in railway car bodies, also using piezoeletric material. Finally, Yan *et al.* (2014) used an electromagnetic shunt to isolate the vibration of a plate by improving the damping force of the structure.

Fatigue phenomenon may occur in any mechanical system due to excessive ambient or operational vibration. It starts with stress accumulation of cyclic loads, resulting in plastic deformations and therefore microscopic cracks that extend

and join together forming large cracks. In extreme cases, these cracks may result in structural failures by nucleation and crack growth (Sobczyk, 1992). The estimation of fatigue life becomes important for structural design, with the damage accumulation methods as the most common decision criterion.

With this information, the paper aims to analyse the behaviour of the shunt circuit coupling in a simple beam structure, to better understand the improvements in a possible operational scenario, that is in a fatigue analysis on the time domain. A resistive shunt circuit and a bimorph beam in series are chosen to compose the structure.

2. ELETROMECHANICAL BASE MODEL

The analyzes in this work consider an analytical model for the vibrations of a cantilevered beam under base transverse excitation. This model is widely used in harvesting analyses, where it is desired to extract vibration from the system in the form of electrical energy through a coupled electrical circuit. In this sense, a bimorph beam (metallic substructure covered with piezoceramic layers), as shown in Fig. 1 , harmonically excited at the base and with a mass at the tip (M_t) was modeled (Erturk, 2011).

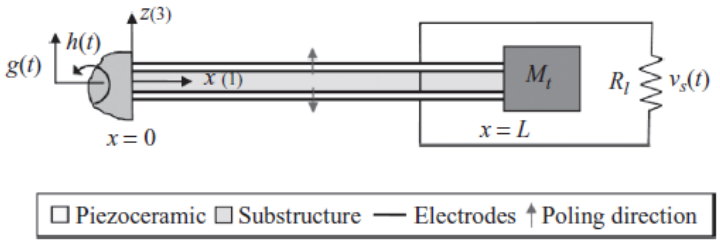

Figure 1. Schematic diagram of the control strategy.

Figure 1 shows the base oscillating in translation ($g(t)$) and rotation ($h(t)$), however, all analyzes performed neglect the rotation excitation. In addition, some model hypotheses are: Euler-Bernoulli beam model with piezoelectric coupling; electromechanically coupled equations for transversely oscillating beams; linear elastic deformations; internal and external damping mechanisms; the substructure and the piezoceramics connection are a perfect bonding; continuous and ideal piezoelectric electrode with negligible thickness; polarization in the 3 direction of the piezoceramics; and the induced electric field is uniform along the length of the beam.

2.1 Dynamic response

Given the assumed hypotheses and the constitutive relations of piezoelectricity, it is possible to write the equation that governs the forced vibration of the system described in Eq. (1) (Erturk, 2011):

$$YI\frac{\partial^4 w(x,t)}{\partial x^4} + c_s I\frac{\partial^5 w_{rel}(x,t)}{\partial x^4 \partial t} + c_a\frac{\partial w_{rel}(x,t)}{\partial t} + m\frac{\partial^2 w_{rel}(x,t)}{\partial t^2} \vartheta v(t)\left[\frac{d\delta(x)}{dx} - \frac{d\delta(x-L)}{dx}\right] = - [m + M_t\delta(x-L)]\frac{\partial^2 w_b(x,t)}{\partial t^2}\,, \tag{1}$$

where YI is the bending stiffness in the short-circuit condition, $w_{rel}(x,t)$ is the transverse displacement of the beam (neutral line) concerning the base at position x and at time t, c_a is the viscous damping coefficient of air, c_s is the strain-rate damping coefficient (it appears as an effective term $c_s I$ for the composite structure) , m is the mass per unit length of the beam, M_t is the tip mass, $\delta(x)$ is the Dirac delta function, ϑ is the backward coupling coefficient (depends if the circuit is connected in series or parallel) and $v(t)$ is the voltage across the electrodes of each piezoceramic layer.

Based on the proportional damping (or modal damping) assumption, the vibration response relative to the base of the bimorph beam can be represented as a convergent series of eigenfunctions:

$$w_{rel}(x,t) = \sum_{r=1}^{\infty} \phi_r(x)\eta_r(t)\,, \tag{2}$$

where $\phi_r(x)$ is the mass-normalized eigenfunction of the *r*th vibration mode, and $\eta_r(t)$ is the modal mechanical coordinate expression of the connection case (series or parallel). These functions have different shapes depending on the boundary and orthogonality conditions. The application of these conditions, detailed by Erturk (2011), allows writing the partial

differential equation of motion as an infinite set of ordinary differential equations. The equivalent electromechanical equations governing the modal mechanical coordinate and the voltage response of a bimorph beam are be given by:

$$\frac{\mathrm{d}^2\eta_r(t)}{\mathrm{d}t^2} + 2\zeta_r\omega_r\frac{\mathrm{d}\eta_r(t)}{\mathrm{d}t} + \omega_r^2\eta_r(t) - \tilde{\theta}_r v(t) = f_r(t)\,, \tag{3}$$

$$C_{\tilde{p}}^{eq}\frac{\mathrm{d}v(t)}{\mathrm{d}t} + \frac{v(t)}{R_l} + \sum_{r=1}^{\infty}\tilde{\theta}_r\frac{\mathrm{d}\eta_r(t)}{\mathrm{d}t} = 0\,, \tag{4}$$

where the modal electromechanical coupling term $\tilde{\theta}_r$ and the equivalent capacitance $C_{\tilde{p}}^{eq}$ depend on the way piezoceramic layers are connected.

The undamped natural frequency of the system of the rth vibration mode is calculated using Eq. 5:

$$\omega_r = \lambda_r\sqrt{\frac{YI}{mL^4}}\,. \tag{5}$$

In possession of the natural frequencies, it is can calculate the damping factor using experimental data of the given material. Other solution is to use the linear system in Eq. 6 and solve it for each mode, assuming at least two initial values and calculating the linear growth of the damping factors. The i and j indexes corresponds to two consecutive vibration mode.

$$\begin{bmatrix} c_s I \\ c_a \end{bmatrix} = \frac{2\omega_j\omega_k}{\omega_j^2 - \omega_k^2}\begin{bmatrix} \dfrac{YI}{\omega_k} & -\dfrac{YI}{\omega_j} \\ -m\omega_k & m\omega_j \end{bmatrix}\begin{bmatrix} \zeta_j \\ \zeta_k \end{bmatrix}\,. \tag{6}$$

Considering an harmonic base displacement ($g(t) = W_0\mathrm{e}^{j\omega t}$), the modal function of forces will also have an harmonic form $f_r(t) = F_r\mathrm{e}^{j\omega t}$. Substituting the steady-state response expressions $\eta_r(t) = H_r\mathrm{e}^{j\omega t}$ and $v(t) = V\mathrm{e}^{j\omega t}$ into Eq. (3) and Eq. (4) gives the coupled linear algebraic equations for the complex terms H_r and V:

$$\left(\omega_r^2 - \omega^2 + j2\zeta_r\omega_r\omega\right)H_r - \tilde{\theta}_r V = F_r\,, \tag{7}$$

$$\left(Y(\omega) + j\omega C_{\tilde{p}}^{eq}\right)V + j\omega\sum_{r=1}^{\infty}\tilde{\theta}_r H_r = 0\,, \tag{8}$$

Isolating the terms of displacement in the two equations, it is possible to obtain an expression for the relative tip displacement:

$$w_{rel}(x,t) = \sum_{r=1}^{\infty}\left[\left(F_r - \tilde{\theta}_r\frac{\displaystyle\sum_{r=1}^{\infty}\frac{j\omega\tilde{\theta}_r F_r}{\omega_r^2 - \omega^2 + j2\zeta_r\omega_r\omega}}{\displaystyle Y(\omega) + j\omega C_{\tilde{p}}^{eq} + \sum_{r=1}^{\infty}\frac{j\omega\tilde{\theta}_r^2}{\omega_r^2 - \omega^2 + j2\zeta_r\omega_r\omega}}\right)\frac{\phi_r(x)\mathrm{e}^{j\omega t}}{\omega_r^2 - \omega^2 + j2\zeta_r\omega_r\omega}\right]\,, \tag{9}$$

where $Y(\omega)$ is the external admittance and depends on the external circuit, and the expressions for resistive and resistive-inductive circuits are presented in Tab. (1) (De Marqui Jr. *et al.*, 2011).

Bauchau and Craig (2009) describes that in the case of symmetrical cross-sections in relation to a plane perpendicular to the neutral plane, the stress on the beam is calculated as:

$$\sigma_{xx}(x) = -\bar{y}Y_s\frac{\mathrm{d}^2 w(x)}{\mathrm{d}x^2}, \tag{10}$$

where $\bar{y}$ is the height of the cross-section of the stress (the maximum stress is $|\bar{y}| = \pm h/2$) and Y_s is the elastic modulus of the material.

Table 1. Admittances for different external circuits.

External circuit	Resistive	Resistive-indutive (series)	Resistive-indutive (parallel)
Admitance	$\frac{1}{R}$	$\frac{1}{R+j\omega L}$	$\frac{1}{R}+\frac{1}{j\omega L}$

Since the relative displacement of the beam described in Eq. 9 only has one term depending of x (the mode shape $\phi(x)$), it becomes clear the calculation of the stress history of the beam coupled with a resistive shunt circuit using the Eq. 11:

$$\sigma_{xx}(x,t) = -\sum_{r=1}^{\infty}\left[\left(F_r - \tilde{\theta}_r \frac{\sum_{r=1}^{\infty}\frac{j\omega\tilde{\theta}_r F_r}{\omega_r^2-\omega^2+j2\zeta_r\omega_r\omega}}{\frac{1}{R}+j\omega C_{\tilde{p}}^{eq}+\sum_{r=1}^{\infty}\frac{j\omega\tilde{\theta}_r F_r}{\omega_r^2-\omega^2+j2\zeta_r\omega_r\omega}}\right)\frac{\mathrm{e}^{j\omega t}}{\omega_r^2-\omega^2+j2\zeta_r\omega_r\omega}\left(\frac{\mathrm{d}^2\phi_r(x)}{\mathrm{d}x^2}\right)\right] Y_s\bar{y}\,. \tag{11}$$

Finally, is possible to calculate the Frequency Response Function of the tip displacement, based on the relative displacement in the end of the beam ($x = L$), by using the Eq. 12, where σ_r is the applied force value:

$$\alpha(L,t) = \frac{w_{rel}(L,t)}{-\omega^2 W_0 \mathrm{e}^{j\omega t}} = \sum_{r=1}^{\infty}\left[\left(\sigma_r - \tilde{\theta}_r \frac{\sum_{r=1}^{\infty}\frac{j\omega\tilde{\theta}_r \sigma_r}{\omega_r^2-\omega^2+j2\zeta_r\omega_r\omega}}{\frac{1}{R}+j\omega C_{\tilde{p}}^{eq}+\sum_{r=1}^{\infty}\frac{j\omega\tilde{\theta}_r^2}{\omega_r^2-\omega^2+j2\zeta_r\omega_r\omega}}\right)\frac{\phi_r(L)}{\omega_r^2-\omega^2+j2\zeta_r\omega_r\omega}\right]. \tag{12}$$

3. FATIGUE

As described in Chen *et al.* (2011), the number of stress cycles a structure can sustain before the occurrence of failure is known as fatigue life N_f, where fatigue strength is the prediction of this life using the characteristic S-N curve alongside the Palmgren-Miner's rule. The S-N curve of a material corresponds of a two-segments curve representing the number of cycles it resists in a determined stress range. These values are calculated using linear regression of experimental data, as seeing in the ABS Rules for building and classing steel vessels (ABS, 2010). The S-N curve can be represented as:

$$\begin{aligned} N\cdot S^{m_{f1}} &= C_{f1}, \quad \text{when } N \le 10^7 \text{ cycles},\\ N\cdot S^{m_{f2}} &= C_{f2}, \quad \text{when } N \ge 10^7 \text{ cycles}, \end{aligned} \tag{13}$$

where N equals the number of loading to failure, S the stress range and $m_{f1}, m_{f2}, C_{f1}, C_{f2}$ the exponents and coefficients of fatigue strength as a characteristic of the material (Chen *et al.*, 2011). An example of a generic S-N curve is shown at Fig. 2, with the correspondence of each stress range and number of cycles.

The Palmgren-Miner's rule, first cited by Palmgren (1924) then combined with Miner's rule, allowed the definition of a cumulative damage in a structure subjected to k different stress ranges S_i ($1 \le 1 \le k$) with n_i cycles each using the Eq. 14, where N_i is the number of loading cycles under the stress range Si in the S-N curve. When the value of the cumulative damage equals to 1, the failure by fatigue occurs.

$$D = \sum_{i=1}^{k}\frac{n_i}{N_i} = 1 \tag{14}$$

The fatigue life can be estimated using the accumulated damage and the time span related to the signal used in the previous calculations. The Eq. 15 describes the fatigue life, where T is the time considered in the analysis.

$$N_f = \frac{T}{D} \tag{15}$$

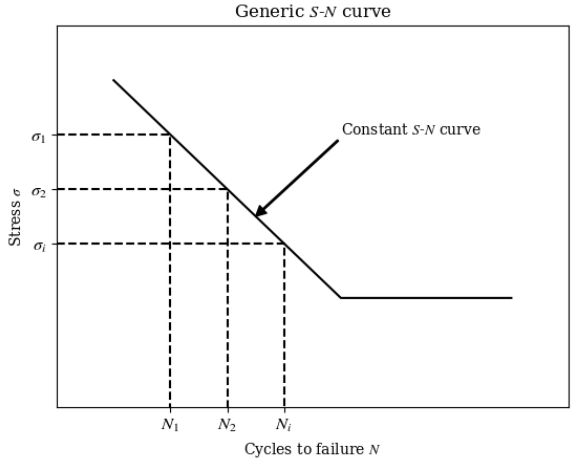

Figure 2. Relation between stress and cycles to failure in a S-N curve.

3.1 Rainflow cycle-counting method

The rainflow method is used to simplify a complex load history into a set of elementary load cycles using de peaks of the signal to do so. It was first proposed by Endo *et al.* (1974), with the signal peaks and valleys rotated to the vertical axis and making an allusion to a pagoda roof with running rain water. Figure 3 shows an example of a signal being counted with the rainflow method (Milne, 2003).

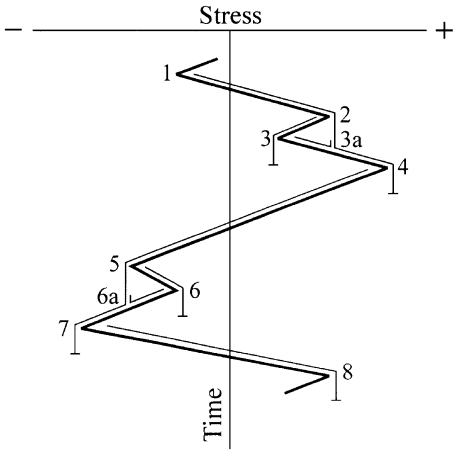

Figure 3. Exemplification of the rainflow cycle-counting method and analogy of the name.

There are three basic rules to the rainflow method: the rainflow starts from each peak or valley, but doesn't start while the rain is flowing down; the rainflow stops when the magnitude of the following peak or valley is equal or larger than the first peak or valley; the rainflow stops when it encounters the pervious rainflow. Every range is counted as a half cycle. When the counted half cycle occurs in pairs of equal magnitudes, it forms a full cycle (Milne, 2003).

4. OPTIMIZATION

The displacement FRF $\alpha(\omega, x)$ holds the information of the shunt circuit influence in the total displacement of the structure. As is already known, the tip displacement of a cantilever beam is directly proportional to the strain and stress present in the structure. Finding the minimum peak value of a certain vibration mode in the displacement FRF gives a value of resistance in the shunt circuit that corresponds to the minimum vibration in the structure. Therefore, this resistance gives the minimum stress in the cross section close to the base, resulting in an optimal model with less stress accumulation in the time domain.

Equation 16 shows the pseudo objective function and the optimization problem. The only decision variable is the resistance of the shunt circuit with a maximum value of $1\mathrm{e}10\ \Omega$. The peaks are considered only for the first vibration mode, and the peaks are defined as any sample whose two direct neighbours have a smaller amplitude. The implementation complexity of the objective function demands the use of Genetic Algorithm to find the solution using Functional

Programming paradigm.

$$\begin{aligned} \min_{R} \quad & \text{peak}[\alpha(\omega, L)] \\ \text{s.t.} \quad & 0 \leq R \leq 1\text{e}10 \end{aligned} \tag{16}$$

5. CASE STUDY

An electromechanical analysis of a bimorph cantilever beam is presented in this section, in order to demonstrate the fatigue life variation of the structure in different scenarios. Piezoceramic fatigue life was not considered in the analysis, as the main purpose of this work is to verify the increase of the fatigue life in the metal structure. The Python programming language was used to perform all the calculations and generating the graphs, and an optimization module called Platypus was used to find the optimal resistance of the circuit.

5.1 Geometric and material properties

The properties of the beam are described in the Tab. 2 for both materials. An aluminum alloy 2024-T3 was chosen to compose the main structure with the fatigue data from Lipski (2016) while the PZT-4 type was selected with data from eFunda (2021). Calculations of the piezoeletric constants are necessary in order to use in this beam formulation, as described in the Eq. 17:

$$\bar{c}_{11}^{E} = \frac{1}{s_{11}^{E}}\,, \qquad \bar{e}_{31} = \frac{d_{31}}{s_{11}^{E}}\,, \qquad \bar{\varepsilon}_{33}^{S} = \varepsilon_{33}^{T} - \frac{d_{31}^{2}}{s_{11}^{E}}\,. \tag{17}$$

Table 2. Geometric and material values of the structure.

	Structure	Piezoceramic
Length (L) (mm)	100	100
Width (b) (mm)	30	30
Thickness (h_s, h_p) (mm)	1	0.3 (each)
Material	Aluminum 2024-T3	PZT-4
Density (ρ_s, ρ_p) (kg/m²)	2780	7500
Elastic modulus (Y_s, $\bar{c}_{11}^{E}$) (GPa)	73.1	81.3
Piezoeletric constant ($\bar{e}_{31}$) (C/m²)	—	-10
Permittivity constant ($\bar{\varepsilon}_{33}^{E}$) (nF/m)	—	12.74
Fatigue constant (C_f)	3.15e14	—
Fatigue exponent (m_f)	4.10	—

After the selection of the base parameter, other initial calculations are necessary in order to calculate the stress history, such as the equivalent stiffness of the structure and the mass per length unit. The value $YI_{eq} = 0.81202\ \text{Nm}^2$ and $m = 0.2184\ \text{kg/m}$ for the present structure are calculated via Eq. 18.

$$YI_{eq} = \frac{2b}{3}\left\{ Y_s \frac{h_s^3}{8} + \bar{c}_{11}^{E}\left[\left(h_p + \frac{h_s}{2} \right)^3 - \frac{h_s^3}{8} \right] \right\}\,, \qquad m = b\left(\rho_s h_s + 2\rho_p h_p\right)\,. \tag{18}$$

5.2 Open and closed circuit results in the time domain

Eight modes were considered for calculating the natural frequency, mode shapes, damping ratios and A_r constant. The solutions of the vibration parameters such as the frequency parameter, natural frequencies and damping factors are presented in the Tab. 3, for each vibration mode. Setting of the theoretical experiment, a frequency of $w = 1.5\ \text{krad/s}$ and a total vertical displacement range of $W_0 = 25.4\ \text{mm}$ were selected in order to excite the base of the structure in a $t = 200\ \text{s}$ time window, respecting the limits of commercial shakers and the time range seen in other similar experiments.

In the time domain, two initial cases are shown in Fig. 4. The open circuit corresponds to 0 resistance, i.e. with no electrical coupling between the shunt circuit and the piezoelectric ceramic. The closed circuit corresponds to a coupling of the shunt circuit with an arbitrary resistance value of $R = 1\text{e}6\ \Omega$. The graphs make it clear the direct influence of the coupling, giving a coherent basis to the vibration attenuation generated by the shunt circuit and the piezoelectric material.

Table 3. Parameters of the structure per vibration mode.

Mode	1	2	3	4	5	6	7	8
Frequency param. (λ_r)	1.41821	4.11011	7.18958	10.29787	13.42054	16.54989	19.68293	22.81821
Natural frequency (ω_r)	61.72479	518.4211	1586.29256	3254.40285	5527.3437	8405.56624	11889.29998	15978.64854
Damping ratios (ζ_r)	0.01000	0.01200	0.03389	0.06900	0.11700	0.17784	0.25151	0.33799

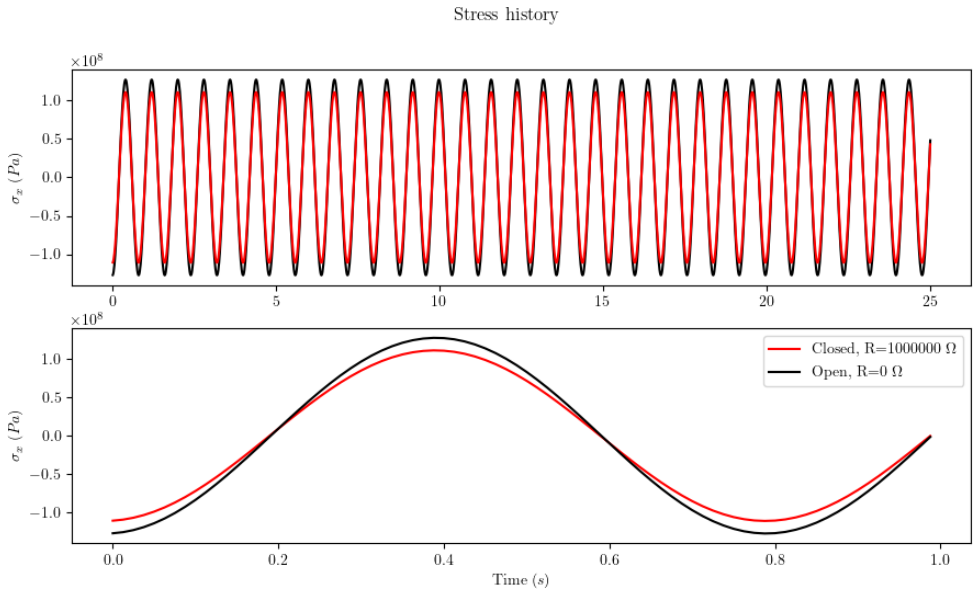

Figure 4. Stress history in the base of the beam (most solicited).

After this, the optimization of the displacement FRF was conducted using a genetic algorithm. Setting the optimization problem with 10,000 function evaluations, the algorithm calculates the optimal resistance equals to $R = 39633.916445\ \Omega$. Figure 5 contains the tip displacement FRF of the structure with a wide range of resistances, including the optimal resistance calculated before. It becomes clear the curve of the optimal peak in comparison to the other values.

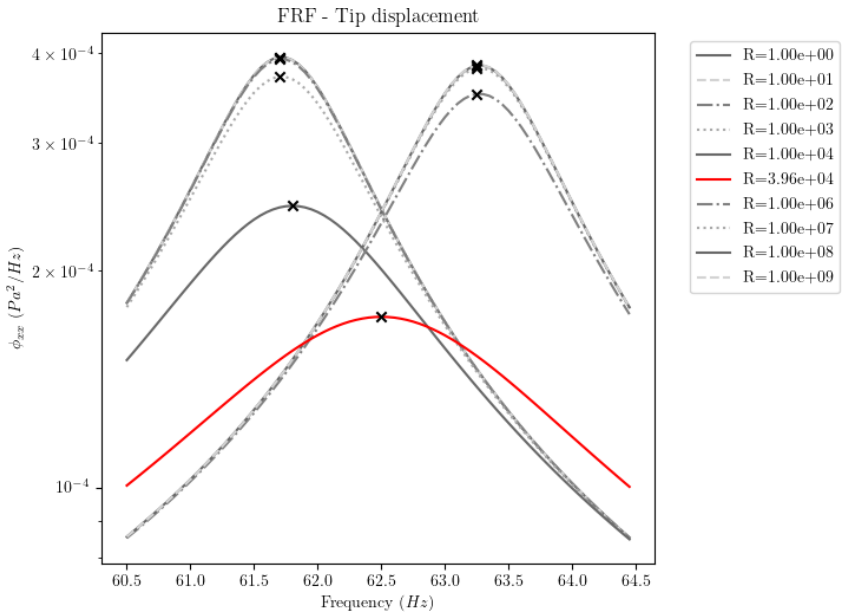

Figure 5. Tip displacement FRF for various cases and the optimal resistance.

Using the same resistance values of before, a fatigue analysis was performed with the rainflow cycle-counting method applied to the stress history. The most solicited part of the beam is right at the fixed support, and the results of the analysis are shown in Fig. 6. The optimal value of resistance consists of the higher fatigue life expectation equals to $N_f = 212.28$ h, which is inversely proportional to the damage and has the lower damage $D = 2.61714\text{e}{-04}$.

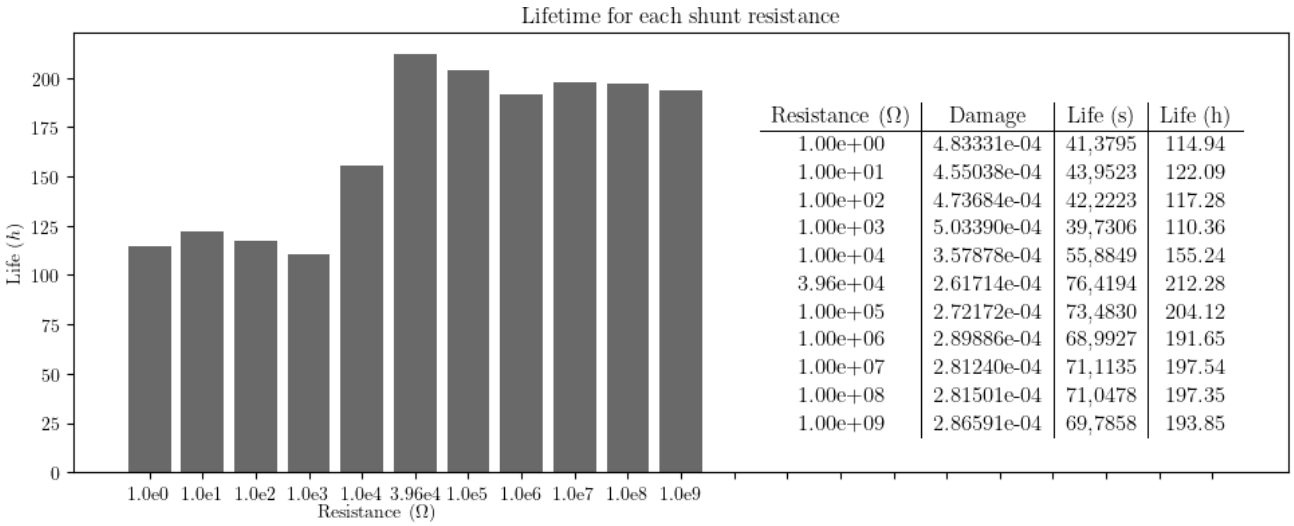

Resistance (Ω)	Damage	Life (s)	Life (h)
1.00e+00	4.83331e-04	41,3795	114.94
1.00e+01	4.55038e-04	43,9523	122.09
1.00e+02	4.73684e-04	42,2223	117.28
1.00e+03	5.03390e-04	39,7306	110.36
1.00e+04	3.57878e-04	55,8849	155.24
3.96e+04	2.61714e-04	76,4194	212.28
1.00e+05	2.72172e-04	73,4830	204.12
1.00e+06	2.89886e-04	68,9927	191.65
1.00e+07	2.81240e-04	71,1135	197.54
1.00e+08	2.81501e-04	71,0478	197.35
1.00e+09	2.86591e-04	69,7858	193.85

Figure 6. Bar chart of the fatigue life in hours and complete results.

6. CONCLUSIONS

After modelling the cantilever beam subjected to base excitation, results show the improvement on fatigue life of a the beam when using the optimal resistance value on the shunt circuit. It proves, through the results, that it is possible to maximize the attenuation of the vibration in a structure when setting up the configurations of the circuit. It also shows the direct relation between the vibration control and the calculation of the uniaxial fatigue life. In short, the contributions of the present work are:

- Extension of the analytical method for a cantilever beam, obtaining the stress history at any given point;
- Comparison between the stress response of the open and close circuit;
- Creation of an optimization problem to minimize the peaks of the FRF;
- Validation of the improvement in fatigue life using the resultant configuration obtained from the optimization problem.

The resistive shunt circuit was an arbitrary choice. Other types of circuits may achieve different or even better results, opening a demand for more complex analysis in different types of structures. It may also be interesting the insertion of geometrical and material parameters in the optimization problem for better design. Finally, the optimization problem may include other objectives, such as maximizing the voltage output for harvesting in parallel of minimizing the accumulated damage.

7. ACKNOWLEDGEMENTS

The authors are grateful to CNPq for the continued support to their research activities through the research grant 306138/2019-0 (A. M. G. de Lima). It is also important to express the acknowledgements to the CAPES and FAPEMIG, especially to the research projects APQ-01865 and PPM-0058-18 (A. M. G. de Lima).

8. REFERENCES

ABS, 2010. *Rules for building and classing steel vessels.* American Bureau of Shipping, Houston.

Bauchau, O.A. and Craig, J.I., eds., 2009. *Structural Analysis*. Springer Netherlands. doi:10.1007/978-90-481-2516-6.

Chen, N.Z., Wang, G. and Soares, C.G., 2011. "Palmgren–miner's rule and fracture mechanics-based inspection planning". *Engineering Fracture Mechanics*, Vol. 78, No. 18, pp. 3166–3182. doi:10.1016/j.engfracmech.2011.08.002.

De Marqui Jr., C., Vieira, W.G.R., Erturk, A. and Inman, D.J., 2011. "Modeling and analysis of piezoelectric energy harvesting from aeroelastic vibrations using the doublet-lattice method". *Journal of Vibration and Acoustics, Transactions of the ASME*, Vol. 133, No. 1, pp. 1–9.

eFunda, 2021. "efunda:piezo material data". http://www.efunda.com/materials/piezo/material_data/matdata_index.cfm. Acessed 10 jun 2021.

Endo, T., Mitsunaga, K., Takahashi, K., Kobayashiand, K. and Matsuishi, M., 1974. "Damage evaluation of metals for random or varying loading - three aspects of rain flow method." *Proceedings Symposium on Mechanical Behavior of Materials*, Vol. 1-2, pp. 371–380.

Erturk, 2011. *Piezoelectric Energy Harvestin*. John Wiley & Sons. ISBN 047068254X.

Gotz, B., Heuss, O., Platz, R. and Melz, T., 2017. "Optimal tuning of shunt parameters for lateral beam vibration attenuation with three collocated piezoelectric stack transducers". *EACS 2016 paper*. doi:10.15131/SHEF.DATA.4206453.V1.

Gripp, J.A.B. and Rade, D.A., 2018. "Vibration and noise control using shunted piezoelectric transducers: A review". *Mechanical Systems and Signal Processing*, Vol. 112, pp. 359–383.

Hansson, J., Takano, M., Takigami, T., Tomioka, T. and Suzuki, Y., 2004. "Vibration suppression of railway car body with piezoelectric elements (a study by using a scale model)". *JSME International Journal Series C*, Vol. 47, No. 2, pp. 451–456. doi:10.1299/jsmec.47.451.

Leo, D.J., 2007. *Engineering Analysis of Smart Material Systems*. John Wiley & Sons, Inc., Hoboken, NJ, USA.

Lipski, A., 2016. "Rapid determination of the wöhler's curve for aluminum alloy 2024-t3 by means of the thermographic method". Author(s). doi:10.1063/1.4965936.

Milne, I., 2003. *Comprehensive structural integrity*. Elsevier/Pergamon, Amsterdam Boston. ISBN 0080437494.

Palmgren, A., 1924. "Die lebensdauer von kugellagern". *Zeitschrift des Vereines Deutscher Ingenieure*, Vol. 68, pp. 339–341.

Sobczyk, K., 1992. *Random fatigue : from data to theory*. Academic Press, Boston. ISBN 0126542252.

Vér, L.I. and Beranek, L.L., 2005. *Noise and Vibration Control Engineering*. John Wiley & Sons, Inc., Hoboken, NJ, USA.

Wright, R.I. and Kidner, M.R.F., 2004. "Vibration absorbers: A review of applications in interior noise control of propeller aircraft". *Journal of Vibration and Control*, Vol. 10, No. 8, pp. 1221–1237.

Yan, B., Zhang, X. and Luo, Y., 2014. "Investigation of negative resistance shunt damping for the vibration control of a plate". *International Journal of Applied Electromagnetics and Mechanics*, Vol. 45, pp. 93–100. ISSN 18758800, 13835416. doi:10.3233/JAE-141817.

9. RESPONSIBILITY NOTICE

The authors are solely responsible for the printed material included in this paper.